

1 **Denitrification kinetics indicates nitrous oxide uptake is unaffected by electron**
2 **competition in Accumulibacter**

3
4 Roy Samarpita^{*}, Pradhan, Nirakar^{**}, NG How Yong^{***}, Wuertz Stefan^{**,****, a}

5
6 ^{*}Singapore Centre for Environmental Life Sciences Engineering, National University
7 of Singapore, Singapore 119077 (Email: samarpita.roy@u.nus.edu)

8 ^{**}Singapore Centre for Environmental Life Sciences Engineering, Nanyang
9 Technological University, Singapore 637551 (Email: nirakar.pradhan@gmail.com)

10 ^{***}NUS Environmental Research Institute, National University of Singapore, 5A
11 Engineering Drive 1, Singapore 117411 (Email: howyongng@nus.edu.sg)

12 ^{****}School of Civil and Environmental Engineering, Nanyang Technological
13 University, Singapore 639798 (Email: swuertz@ntu.edu.sg)

14

15

16

17

18

19

20

21

22 ^aCorresponding author:

23 Stefan Wuertz (swuertz@ntu.edu.sg), Singapore Centre for Environmental Life

24 Sciences Engineering, Nanyang Technological University, Singapore

25 **ABSTRACT**

26 Denitrifying phosphorus removal is a cost and energy efficient treatment technology
27 that relies on polyphosphate accumulating organisms (DPAOs) utilizing nitrate or
28 nitrite as terminal electron acceptor. Denitrification is a multistep process and many
29 organisms do not possess the complete pathway, leading to the accumulation of
30 intermediates such as nitrous oxide (N₂O), a potent greenhouse gas and ozone
31 depleting substance. *Candidatus* Accumulibacter organisms are prevalent in
32 denitrifying phosphorus removal processes and, according to genomic analyses,
33 appear to vary in their denitrification abilities based on their lineage. Yet,
34 denitrification kinetics and nitrous oxide accumulation by Accumulibacter after long-
35 term exposure to either nitrate or nitrite as electron acceptor have never been
36 compared. We investigated the preferential use of the nitrogen oxides involved in
37 denitrification and nitrous oxide accumulation in two enrichments of Accumulibacter
38 and a competitor – the glycogen accumulating organism *Candidatus* Competibacter.
39 A metabolic model was modified to predict phosphorus removal and denitrification
40 rates when nitrate, nitrite or N₂O were added as electron acceptors in different
41 combinations. Unlike previous studies, no N₂O accumulation was observed for
42 Accumulibacter in the presence of multiple electron acceptors. Electron competition
43 did not affect denitrification kinetics or N₂O accumulation in Accumulibacter or
44 Competibacter. Despite the presence of sufficient internal storage polymers
45 (polyhydroxyalkanoates, or PHA) as energy source for each denitrification step, the
46 extent of denitrification observed was dependent on the dominant organism in the
47 enrichment. Accumulibacter showed complete denitrification and N₂O utilization,
48 whereas for Competibacter denitrification was limited to reduction of nitrate to nitrite.

49 These findings indicate that DPAOs can contribute to lowering N₂O emissions in the
50 presence of multiple electron acceptors under partial nitrification conditions.

51

52 **Keywords**

53 Nitrous oxide (N₂O) emission, Accumulibacter, electron competition, free nitrous
54 acid, polyhydroxyalkanoates

55 1. INTRODUCTION

56 Biological nutrient removal processes are regarded as cost-effective,
57 sustainable solutions to tackle excess carbon, phosphorus (P) and nitrogen (N) in
58 wastewater. However, complete P and N removal usually requires high aeration,
59 accounting for more than 60% of the overall power consumption at a wastewater
60 treatment plant (WWTP) [1]. To meet rigorous effluent discharge limits, external
61 carbon dosage is often required to achieve complete denitrification resulting in
62 increased operational costs [2]. In this regard, denitrifying phosphorus removal (DPR)
63 has been identified as an optimal treatment solution due to its reduced energy
64 consumption, sludge wastage and carbon requirement for nutrient removal.

65 In the DPR process, sludge is cycled through anaerobic-anoxic conditions
66 allowing denitrifying phosphorus accumulating organisms (DPAOs) such as
67 *Candidatus Accumulibacter phosphatis* (hereafter referred to as Accumulibacter) to
68 take up organic carbon under anaerobic conditions by utilizing stored polyphosphate
69 as a source of energy. In the subsequent anoxic phase, electron acceptors such as
70 nitrate or nitrite are reduced to meet growth and metabolic requirements [3-5]. These
71 conditions also lead to the growth of denitrifying glycogen accumulating organisms
72 (DGAOs), which compete with DPAOs for organic carbon under anaerobic
73 conditions, but do not aid in phosphorus removal in the subsequent phase; hence
74 recognized as competitors to DPAOs. *Candidatus Competibacter phosphatis*
75 (hereafter referred to as Competibacter) is one such DGAO commonly found in
76 laboratory- and full-scale studies [6-9].

77 In terrestrial and aquatic ecosystems, the conversion of nitrous oxide
78 (N_2O) to nitrogen gas ($E^{\circ} = +1.35$ V at pH 7) by nitrous oxide reductase (Nos) is the
79 only known biological N_2O attenuation process in the biosphere [10, 11]. Genomic

80 evidence revealed that many organisms possess only a subset of this denitrification
81 pathway, sometimes lacking the nitrous oxide reductase gene (*nos*), resulting in the
82 accumulation of N₂O [11, 12]. This is particularly important in engineered systems
83 such as WWTPs where denitrification is implemented to remove nitrogen from
84 influent wastewater [13, 14]. To this end, a genomic comparison of the denitrification
85 pathway in *Accumulibacter* clades IA, IIA, IIB, and IIC showed significant
86 differences and suggested that some clades were incapable of reducing N₂O [15-17].
87 Likewise, there is evidence that phylogenetically similar members of *Competibacter*
88 have distinct denitrification capabilities [7, 18-20]. However, most metabolic models
89 ignore the differences in denitrification capabilities of PAOs and GAOs and split the
90 total nitrogen reduced between anoxic and aerobic phases [21-24]. Such an approach
91 overlooks differences in phosphorus removal rates by different *Accumulibacter* clades
92 that arise due to affinity towards certain nitrogen oxides. In addition to differences in
93 denitrification abilities, environmental factors have been associated with increased
94 N₂O release from WWTPs [24-27]. For heterotrophic organisms, studies
95 demonstrated that the presence of nitrogen oxides (i.e., nitrate or nitrite) coupled with
96 free nitrous acid (FNA) accumulation had a negative effect on the nitrous oxide
97 reduction potential [28]. Nitrous oxide accumulation is also affected by electron
98 competition, which results in a higher flow of electrons to one step of the
99 denitrification pathway, rather than electrons being distributed to all denitrification
100 enzymes [25, 28, 29]. In the context of *Accumulibacter*, slow polyhydroxyalkanoates
101 (PHA) degradation has often been reported as a reason for N₂O release from DPR
102 systems, although others have been unable to establish a link between the two [30,
103 31]. Thus, it is unclear whether N₂O emission from the DPR process is due to

104 environmental factors or an incomplete denitrification pathway in dominant
105 denitrifying organisms.

106 Metabolic models have been widely used to predict nutrient removal in
107 wastewater treatment [21-23, 32]. So far, models predicting N₂O accumulation have
108 been developed solely based on external nitrate dosage as terminal electron acceptor
109 [18, 33-36]. However, various additional nitrogen oxides (NO_x) occur simultaneously
110 in biological wastewater treatment, and each can serve as terminal electron acceptor.
111 This necessitates validation of metabolic models to evaluate electron competition and
112 denitrification kinetics in organisms utilizing PHA. The preference for different NO_x
113 has also been shown to affect oxidative phosphorylation and phosphorus transport
114 across cell membranes [26, 36, 37]. Consequently, it is necessary to consider
115 differences in the denitrification pathway and the effect of specific long-term
116 enrichment conditions (nitrate or nitrite as electron acceptor) in modelling
117 approaches.

118 In this study, we compared the denitrification kinetics of two *Accumulibacter*
119 enrichments acclimated to different anoxic conditions. We tested the effect of electron
120 competition on nitrous oxide accumulation in the presence of multiple electron
121 acceptors. These results for *Accumulibacter* were contrasted with denitrification
122 characteristics of a *Competibacter* enrichment. The objectives were to (i) identify any
123 accumulation of intermediates in the denitrification process that would signify a
124 preference for certain terminal electron acceptors, (ii) compare the role of electron
125 competition in nitrous oxide accumulation, and (iii) validate an existing metabolic
126 model to predict the mechanism of phosphorus uptake and nitrogen oxide
127 accumulation in the presence of multiple electron acceptors. We investigated three
128 electron acceptors (nitrate, nitrite and nitrous oxide) dosed in seven different

129 combinations under similar test conditions for all enrichments. We hypothesized that
130 the preference for certain NO_x compounds would be driven either by electron
131 competition or the extent of denitrification performed by the dominant organism in
132 each enrichment culture.

133

134 **2. MATERIALS AND METHODS**

135 *2.1. Reactor operation for enrichment cultures*

136 We operated three lab-scale aerobic granular sludge sequencing batch reactors
137 (SBRs), each with a 2-L working volume and 200 mL headspace, to obtain
138 *Accumulibacter* and *Competibacter* enrichments. *Accumulibacter* was adapted to
139 nitrate or nitrite as terminal electron acceptor under anoxic conditions leading to two
140 different enrichments, *Accumulibacter*_{nitrate} and *Accumulibacter*_{nitrite}, respectively. The
141 third reactor enriched *Competibacter* fed with nitrate under anoxic conditions. The
142 reactors were maintained at a constant temperature of 30°C using a heating jacket,
143 and a cycle length of 6 h consisting of 30 min feeding, 60 min anaerobic react, 120
144 min anoxic react, 120 min aerobic react, 10 min settling and 20 min effluent discharge
145 phases. During the anaerobic phase, 1 L of synthetic feed containing acetate and
146 propionate (3:1 ratio on the basis of total influent chemical oxygen demand, or COD)
147 as carbon source was pumped into each reactor at a rate of 33.33 mL/min.

148 Nitrogen gas was sparged from the bottom of the reactor at 2.0 L/min to
149 provide sufficient mixing during the reaction phases and maintain anaerobic
150 conditions. Subsequently, in the anoxic phase nitrite or nitrate were fed in pulses.
151 Nitrite and nitrate dosages were carefully adjusted to avoid their accumulation in the
152 anoxic phase because this could affect microbial activity in the reactors. During the
153 effluent discharge phase, 1 L of effluent was pumped out of the reactors, leading to a

154 hydraulic retention time of 12 h and a volumetric exchange ratio of 50%. For each
155 cycle, the pH was controlled at 7.5 to 8.0 with 0.5 M NaOH or 0.5 M HCl solution,
156 and the dissolved oxygen (DO) concentration in the aerobic phase was varied from 1
157 to 1.5 mg O₂/L. A programmable logic controller was linked to a SCADA interface
158 for data visualization and storage. The bioreactors were assumed to be at pseudo-
159 steady state at the start of the batch tests as no significant changes in mixed liquor
160 volatile suspended solids (MLSS), volatile suspended solids (VSS) and phosphorus
161 concentrations were observed for three consecutive solids retention times (SRTs).
162 Cycle studies were performed regularly and samples were taken during each phase to
163 monitor reactor performance. The operating conditions for the *Accumulibacter*_{nitrite},
164 *Accumulibacter*_{nitrate} and *Competibacter* enrichment reactors were as follows:

165 **Case 1: *Accumulibacter*_{nitrite}.** A lab-scale aerobic granular sludge SBR operated at
166 30°C and fed with synthetic wastewater in which the influent carbon source was a
167 mixture of acetate and propionate (3:1 ratio for acetate and propionate on the basis of
168 total influent COD) was used to enrich *Accumulibacter*. The synthetic wastewater
169 consisted of 0.15 L solution A and 0.85 L solution B. Solution A (per litre) contained
170 3.5 g NaAc.3H₂O and 0.7 mL of 99.5% propionic acid as the carbon source, 1.20 g
171 MgSO₄.7H₂O, 0.19 g CaCl₂.2H₂O, 1.02 g NH₄Cl, 0.01 g peptone, 0.01 g yeast and 4
172 mL of trace metals solution. The trace metals solution was prepared as described in
173 Smolders et al. (1994) and consisted (per litre) of 0.15 g H₃BO₃, 1.5 g FeCl₃.6H₂O,
174 0.18 g KI, 0.12 g MnCl₂.4H₂O, 0.15 g CoCl₂.6H₂O, 0.06 g Na₂MoO₄.2H₂O, 0.03 g
175 CuSO₄.5H₂O, 0.12 g ZnSO₄.7H₂O and 10 g Ethylenediamine tetra-acetic acid
176 (EDTA). Solution B contained 132 mg K₂HPO₄/L and 103 mg KH₂PO₄/L.
177 Nitrification was inhibited by the addition of 2.38 mg allyl-N thiourea (ATU) per litre
178 feed. After feeding, the mixed liquor contained 12 mg NH₄-N/L, 300 mg COD/L and

179 15 mg PO₄-P/L resulting in a COD to P ratio of 20:1. The anoxic phase was initiated
180 by adding NaNO₂ solution in pulses such that the total concentration in the reactor
181 after each pulse was 10 mg NO₂-N/L. The SRT varied from 12 to 15 d to maintain an
182 MLSS between 2 and 2.5 g/L.

183 **Case 2: Accumulibacter_{nitrate}.** Accumulibacter was enriched at 30°C in a lab-scale
184 aerobic granular sludge SBR using the same enrichment protocol and synthetic
185 wastewater as mentioned in Case I, Accumulibacter_{nitrite}. The only difference in
186 operation of this reactor was that the anoxic phase was initiated by adding KNO₃
187 solution in pulses such that the final concentration in the reactor after each pulse was
188 15 mg NO₃-N/L.

189 **Case 3: Competibacter.** Enrichment of Competibacter was achieved in a lab-scale
190 aerobic granular sludge SBR operated at 30°C with synthetic feed containing acetate
191 as sole carbon source. The synthetic wastewater was similar to that outlined for Case I
192 (Accumulibacter_{nitrite}) with the difference that solution A contained 8.5 g NaAc.3H₂O
193 and solution B contained trace amounts of K₂HPO₄ and KH₂PO₄, such that the
194 resulting phosphorus concentration in the reactor after feeding was 2 mg P/L. After
195 feeding, the mixed liquor contained 300 mg COD/L, 12 mg NH₄-N/L and 2 mg PO₄-
196 P/L resulting in a COD:P of 150:1. The reactor operation phases were similar to those
197 of the other reactors and KNO₃ solution was introduced as a pulse into the reactor
198 during the anoxic phase, resulting in a final concentration in the reactor after each
199 pulse of 15 mg NO₃-N/L.

200

201 2. 2. *Batch tests to measure denitrification kinetics and N₂O accumulation*

202 A total of seven batch tests were performed under different terminal electron acceptor
203 conditions for all enrichments. At the start of each batch test, mixed liquor was

204 withdrawn from the reactor after completion of the anaerobic phase and immediately
205 transferred to batch reactors with nitrogen gas sparging for 5 min to remove trace
206 oxygen. The batch reactors had a total volume of 1.1 L and a working volume of 1 L.
207 The reactor headspace was minimized in order to reduce stripping of nitrous oxide.
208 For all tests, pH was controlled at 8.0 ± 0.1 using 0.5M HCl or 0.5M NaOH for
209 *Accumulibacter* enrichments and 0.2M HCl or 0.2M NaOH for the *Competibacter*
210 enrichment. Nitrous oxide reduction can be severely affected by FNA concentrations
211 as low as $0.7 \mu\text{g HNO}_2\text{-N/L}$ [37]. The aforementioned pH set-point was maintained
212 during the batch tests to reduce susceptibility of sludge to the inhibitory effects of
213 FNA. Once the tests began, no nitrogen was sparged in the batch reactor to minimize
214 N_2O stripping, and the mixed liquor was stirred slowly at a rate of 30 rpm to avoid
215 oxygen intrusion. Dissolved N_2O concentrations were monitored with an online N_2O
216 microsensor (N_2O -R, Unisense A/S, Denmark). Fresh stock of N_2O solution prepared
217 by sparging Milli-Q water with 100% N_2O gas for 5 min at room temperature (24-
218 25°C) was used to calibrate the N_2O probe as per the product instruction manual. N_2O
219 reduced at the cathode of the microsensor produced a current that was converted into
220 a signal by the Picoammeter, and these readings were collected every second.

221 Different combinations of terminal electron acceptors were added for batch
222 tests with the enrichment cultures (Table 1). In each test, nitrogen oxides were added
223 as a pulse such that their concentrations in each batch test reactor ranged from 12 to
224 $15 \text{ mg NO}_x\text{-N/L}$. Four control tests were carried out in duplicate to determine the loss
225 of N_2O due to stripping or other abiotic phenomena. The losses were averaged and
226 deducted from all Picoammeter readings to obtain the true biological N_2O uptake as
227 shown in the supplementary information (Appendix 2). The tests were conducted for
228 30 min and mixed liquor samples for nutrient analysis were collected every 5 min.

229 The MLVSS concentration was measured in triplicate before the start of each batch
230 test and all batch tests were carried out in duplicate. Apparent biomass-specific
231 reduction rates for all nitrogen oxides, electron consumption and distribution rates
232 were calculated in duplicate as outlined in previous studies (SI, Appendix 2). Detailed
233 analytical methods for measuring phosphate, ammonium, nitrite, nitrate, VFA, PHA
234 and glycogen have been outlined in the Supplementary Information (Appendix 1).
235 GraphPad Prism (v6) was used for all statistical analyses.

236

237 2. 3. *DNA extraction, sequencing library preparation, 16S amplicon sequencing* 238 *and analysis*

239 For microbial community analysis, 2 mL of mixed liquor from the three lab-scale
240 reactors was collected on day 0 and day 28, coinciding with the first and last day of
241 the batch tests. The genomic DNA extraction protocol can be found in the SI,
242 Appendix 1. The library pool was sequenced at the Singapore Centre for
243 Environmental Life Sciences Engineering (SCELSE) sequencing facility on a MiSeq
244 (Illumina, US) using MiSeq Reagent kit V3 (2×300 paired end). Sequenced sample
245 libraries were processed according to published DADA2 pipelines using the *dada2* R
246 package (v 1.14). Details of the raw reads processing and community analysis are also
247 explained in details in the SI, Appendix 1.

248

249 2.4 *Model details*

250 It is well established that during the anoxic phase in DPR systems, nitrate, nitrite or
251 nitrous oxide are utilized as terminal electron acceptor by *Accumulibacter* for
252 replenishment of its polyphosphate base, growth and other metabolic activities. The
253 utilization rate of these terminal electron acceptors in *Accumulibacter* is associated

254 with the PHA consumption rate for anoxic growth and subsequent phosphorus uptake.
255 Thus, each step of the denitrification pathway (from NO_3^- to N_2 via NO_2^- , NO and
256 N_2O) can be associated with anoxic growth and phosphorus uptake rates. The model
257 developed by Liu et al. (2015) incorporates these features to evaluate electron
258 competition and nitrous oxide accumulation during denitrifying phosphorus removal
259 [35]. In this study, we extended the application of the model by considering the
260 simultaneous availability of multiple electron acceptors.

261 Each sequentially occurring denitrification step was associated with individual
262 reaction-specific kinetics, i.e., anoxic growth rate on nitrate (μ_{DPAO1}), nitrite (μ_{DPAO2}),
263 and nitrous oxide (μ_{DPAO4}) and their associated phosphorus uptake rates. Experimental
264 data from the batch tests were used to calibrate the relevant reactions and
265 relationships for Accumulibacter enrichments, polyphosphate (X_{PP}), PHAs (X_{PHA}),
266 DPAOs (X_{DPAO}), residual inert biomass (X_{i}) and seven soluble compounds -
267 phosphate (S_{PO4}), nitrate (S_{NO3}), nitrite (S_{NO2}), nitric oxide (S_{NO}), nitrous oxide (S_{N2O}),
268 nitrogen gas (S_{N2}) and readily degradable substrate (S_{s}). The saturation constants for
269 polyphosphate storage ($K_{\text{PP,DPAO}}$, $K_{\text{max,DPAO}}$) and PHA storage (K_{PHA}) incorporated the
270 relative abundance of DPAOs as assessed by 16S rRNA amplicon sequencing. The
271 stoichiometry, component definition, model fitting parameters for Accumulibacter_{nitrite}
272 and Accumulibacter_{nitrate}, composition matrix and kinetic rate expression matrix and
273 literature references are presented in the SI, Appendix 3.

274

275 **3. RESULTS AND DISCUSSION**

276 *3.1 Reactor performance and microbial community characterization*

277 Nutrient concentration measurement and microbial community analysis of the
278 enrichments were conducted regularly. 16S rRNA gene amplicon sequencing was

279 followed by classification of the most abundant ASVs at the highest level of
280 resolution using the SILVA database to determine the degree of enrichment of target
281 organisms and assess whether the community had undergone major shifts during the
282 batch tests (Figure 1). The community structure was complex in all enrichments,
283 although a significant proportion of the microbial community consisted of target
284 organisms along with a low abundance of known competitor organisms.
285 *Accumulibacter*_{nitrate} and *Accumulibacter*_{nitrite} had $48 \pm 4\%$ and $39 \pm 3\%$ relative
286 abundance of target organisms, respectively, and a comparatively lower abundance of
287 *Competibacter* ($< 4\%$ relative abundance). The *Competibacter* enrichment during the
288 batch tests had a relative abundance of $44 \pm 4\%$ target organisms and $6 \pm 3\%$ of
289 *Accumulibacter*. Organisms not known to display PAO or GAO phenotypes detected
290 in the reactors were related to *Thiothrix*, *Thiobacillus*, *Hyphomicrobium*, *SJA-28*,
291 *Denitratisoma*, *Cyanobacteria* and *Terrimonas*; they were approximately fourfold less
292 abundant than target organisms.

293 After an acclimation period lasting one month, pseudo-steady state activity
294 and nitrogen removal was observed for *Accumulibacter*_{nitrite}, *Accumulibacter*_{nitrate} and
295 *Competibacter*-enriched sludge. During the anaerobic feeding phase, VFA was
296 completely consumed followed by an increase in intracellular PHA content in all
297 enrichments (Figure 2). Nitrogen oxides were utilized as terminal electron acceptors
298 with concomitant phosphorus uptake in *Accumulibacter*_{nitrite} and *Accumulibacter*_{nitrate}
299 enrichments. In the anoxic phase, *Accumulibacter*_{nitrite} showed 99% nitrite removal
300 efficiency along with an anoxic phosphorus removal efficiency of 20%, whereas
301 *Accumulibacter*_{nitrate} showed 72% nitrate removal efficiency with an anoxic
302 phosphorus removal efficiency of 10%. The phosphorus remaining at the end of the
303 anoxic phase in both enrichment reactors was utilized rapidly in the subsequent

304 aerobic phase (Figure 2a, b). For *Competibacter*, the reducing power for PHA
305 formation was obtained through glycolysis; therefore, glycogen reduction was
306 observed with a concomitant increase in intracellular PHA in the anaerobic phase
307 (Figure 2c). In the subsequent anoxic phase, nitrate added to the reactors was utilized
308 to replenish the intracellular glycogen levels. The phosphorus concentration did not
309 change during the entire cycle and remained below 1.5 mg/L.

310 The microbial community of *Accumulibacter* enrichments utilized in previous
311 studies included a significant fraction of GAOs, which could have led to confounding
312 factors in understanding the denitrification kinetics of the target organism [26, 35-38].
313 In this study, we performed batch studies with *Accumulibacter* and *Competibacter*
314 enrichments dominated by the target organisms to improve our understanding of their
315 true denitrifying abilities.

316

317 *3.2 Denitrification kinetics with single terminal electron acceptors*

318 To test the denitrification kinetics and propensity for N₂O accumulation in
319 *Accumulibacter*_{nitrate}, *Accumulibacter*_{nitrite} and *Competibacter* enrichments, true
320 nitrous oxide, nitrate and nitrite reduction rates were measured in batch tests A, B and
321 C, respectively (Figure 3a, b, c). These rates were calculated from the observed
322 nitrogen oxide (NO_x) concentration during each test (SI, Appendix 2). A linear
323 decrease in NO_x concentrations was observed in tests with a single terminal electron
324 acceptor, indicating denitrification activity (Fig S1).

325 In batch test A, nitrous oxide reduction rates for *Accumulibacter*_{nitrite} and
326 *Accumulibacter*_{nitrate} enrichments were 7.3 ± 0.43 and 10.6 ± 0.007 mg N gVSS⁻¹ h⁻¹,
327 respectively. These rates were significantly higher than that of *Competibacter* ($p <$
328 0.05). Previously, it had been hypothesized that denitrification using PHA leads to

329 N₂O emissions [25, 39]. Yet, neither experimental nor modelling studies found any
330 evidence to support this claim, suggesting other factors such as pH, free nitrous acid
331 concentration and excess aeration as causes for increased N₂O emissions [26, 34, 40,
332 41]. It is interesting that we observed higher nitrous oxide (N₂O) utilization rates by
333 *Accumulibacter* than by *Competibacter*, despite similar PHA storage and anoxic PHA
334 utilization rates (Table 4). This rules out the possibility of incomplete denitrification
335 and nitrous oxide accumulation solely due to PHA serving as carbon source [13].

336 For batch test B, nitrate reduction rates for *Accumulibacter*_{nitrate} and
337 *Competibacter* were 10.9 ± 0.3 and 5.03 ± 0.39 mg N gVSS⁻¹ h⁻¹, respectively. These
338 reduction rates were significantly higher ($p < 0.05$) than that of *Accumulibacter*_{nitrite},
339 indicating that *Accumulibacter* acclimated to nitrite was less efficient in reducing
340 nitrate. Also, as nitrate was reduced, nitrite accumulation was observed only for the
341 *Competibacter* enrichment. In batch test C, the nitrite reduction rates for
342 *Accumulibacter*_{nitrite} and *Accumulibacter*_{nitrate} were 9.1 ± 0.8 and 10.7 ± 1.2 mg N
343 gVSS⁻¹ h⁻¹, respectively, which was almost six times higher than that observed for
344 *Competibacter*. The preferential utilization of nitrate by *Competibacter* with
345 concomitant nitrite accumulation was also observed in cycle studies, where the anoxic
346 reaction phase was longer than in the batch test (Figure 1c). These differences in
347 nitrite reduction between the enrichments support the conclusion that *Competibacter*
348 had a lower preference for nitrite than *Accumulibacter* ($p < 0.05$).

349 Previously, McIlroy et al. (2015) reported genomes of two *Competibacter*
350 GAOs (*Ca. Competibacter denitrificans* and *Ca. Contendobacter odensis*) encoding
351 different denitrification pathways [7]. *Ca. denitrificans* encodes the complete
352 denitrification pathway, while *Ca. odensis* only encodes genes for nitrate to nitrite
353 reduction. Another study provided evidence of *nos* gene expression in denitrifying

354 communities dominated by *Ca. Competibacter denitrificans*, signifying its active role
355 in N₂O reduction [27]. Consistent with our physiological data, the *Competibacter*
356 enrichment was dominated by members of a *Competibacter*-lineage that could
357 predominantly reduce nitrate to nitrite, and showed limited N₂O uptake despite
358 adequate PHA storage. Genomic analyses of various *Accumulibacter* clades have
359 revealed that most members encode the *nos* gene, and have the potential to utilize
360 N₂O as an electron acceptor [16]. This was reflected in batch tests where adequate
361 N₂O reduction was observed in *Accumulibacter* enrichments. Thus, in addition to
362 adequate environmental conditions required to drive N₂O reduction, enzymatic
363 regulation of the *nos* gene is important in PHA-driven denitrification.

364

365 *3.3 Denitrification kinetics with multiple terminal electron acceptors*

366 Multiple electron acceptors were simultaneously added in batch tests D to G, and the
367 observed NO_x reduction rates were compared with those from the single electron
368 acceptor batch experiments (tests A, B and C). The tests allowed us to investigate the
369 potential for electron competition limiting N₂O utilization with different combinations
370 of terminal electron acceptors for *Accumulibacter* and *Competibacter*. The overall
371 NO_x reduction rates for the *Accumulibacter* and *Competibacter* enrichments increased
372 in the presence of multiple electron acceptors, and were not affected by the
373 simultaneous addition of nitrogen oxides (Figure 3). In a previous study, another
374 phosphorus accumulating organism, *Tetrasphaera*, had shown reduced denitrification
375 kinetics when multiple electron acceptors were added simultaneously, indicating a
376 limited electron supply to different denitrification enzymes [42]. In this study, we
377 observed the opposite with an increase in overall NO_x reduction rates in the presence
378 of multiple electron acceptors, suggesting the absence of electron competition.

379 In batch test D, when nitrite and nitrate were added together as terminal
380 electron acceptors, the nitrate reduction rate was significantly higher for
381 *Accumulibacter*_{nitrate} compared to *Accumulibacter*_{nitrite} ($p < 0.0005$). For both
382 *Accumulibacter* enrichments, the net nitrite reduction rate was observed to be two to
383 five times higher than the net nitrate reduction rate, with no observed N₂O
384 accumulation, suggesting that the *Accumulibacter* taxa enriched in both reactors were
385 able to take up nitrite provided externally as an electron acceptor, despite the
386 simultaneous presence of nitrate. By comparison, for *Competibacter*, the true nitrate
387 reduction rate was twice the true nitrite reduction rate, leading to accumulation of
388 nitrite (Figure 3). The *Competibacter* enrichment displayed preferential utilization of
389 nitrate despite the simultaneous presence of equimolar amounts of nitrate and nitrite,
390 reinforcing our observations from the batch tests of its limited nitrite utilization
391 ability.

392 In batch test E, when nitrate and N₂O were utilized as terminal electron
393 acceptors, the N₂O utilization rate for *Accumulibacter*_{nitrite} was twice its nitrate
394 utilization rate. In contrast, for *Accumulibacter*_{nitrate}, the nitrate, nitrite and N₂O
395 reduction rates were similar, and complete denitrification was observed. However,
396 unlike *Accumulibacter*_{nitrite} the externally provided N₂O was not utilized despite
397 similar PHA levels. This is also reflected in the electron consumption profiles for
398 batch test E (Figure 4), where *Accumulibacter*_{nitrate} showed an equal fraction of
399 electrons consumed during each denitrification step, while in *Accumulibacter*_{nitrite}
400 most electrons were consumed for nitrate and N₂O reduction. When nitrite and N₂O
401 were added together (batch test F, Figure 4), *Accumulibacter*_{nitrite} showed N₂O uptake
402 in excess of that expected by denitrification of nitrite; by comparison,
403 *Accumulibacter*_{nitrate} exhibited similar nitrite and N₂O reduction rates with no excess

404 N₂O uptake. Finally, in batch test G where nitrate, nitrite and N₂O were added
405 together, the total denitrification rate for both *Accumulibacter* enrichments was 1.5 to
406 2 times higher than that of *Competibacter*.

407 In comparison to previous studies measuring denitrification kinetics in DPAOs
408 and DGAOs, nitrous oxide accumulation was not observed in this study when
409 multiple electron acceptors were added simultaneously (Table 2) [36, 43]. FNA
410 concentrations in previous studies ranged from 0.001 to 0.015 mg HNO₂-N L⁻¹, which
411 is much higher than the suggested inhibitory concentrations of 0.0007 – 0.001 mg
412 HNO₂-N L⁻¹ [26]. FNA in excess of inhibitory concentrations has been shown to
413 affect the *nos* gene transcriptional process, and directly react with the copper-
414 containing active sites of N₂O reductase (Nos) [44, 45]. Therefore, in this study, the
415 pH and NO_x dosage study were adjusted such that the FNA formed was below the
416 inhibitory levels (0.1 – 0.2 µg HNO₂-N L⁻¹). It has also been proposed that the limited
417 bioenergetic advantage of N₂O reduction for a cell reducing nitrate to nitrogen gas
418 (i.e., ~20% of the total energy generated) allows for release of N₂O as the final
419 denitrification product instead of N₂ [29]. Further, utilizing N₂O produced within a
420 cell generates more energy than transporting N₂O into the cell and subsequently
421 reducing it to nitrogen gas [42]. However, in this study, we observed that
422 *Accumulibacter* was able to utilize N₂O that was externally provided in addition to
423 N₂O produced as a result of denitrification of NO_x. The electron distribution patterns
424 for *Accumulibacter*, too, indicated a significant portion of electrons was consumed by
425 Nos, which was not limited by the simultaneous presence of other NO_x (SI, Fig S3).
426 Although the gene expression levels of various denitrification enzymes involved were
427 not measured in this study, previous studies have identified a strong correlation

428 between the transcription of *nosZ* genes (clade I and II) and the N₂O reduction rate
429 [10, 27].

430 It is likely that a combination of factors such as adequate intracellular PHA
431 storage, higher availability of N₂O and low FNA inhibition in this study allowed for
432 adequate *nos* transcription. This made it bioenergetically feasible for *Accumulibacter*
433 to transport and reduce externally added N₂O, while simultaneously utilizing N₂O
434 produced by nitrate or nitrite reduction.

435

436 *3.4 Electron consumption and distribution during denitrification*

437 For the batch tests conducted, we compared electron consumption and distribution
438 trends as they have been previously shown to be affected by electron competition
439 [28]. Here, *Accumulibacter* enrichments were observed to have a higher electron
440 consumption rate than *Competibacter*, which can be attributed to higher
441 denitrification rates observed in the former. The total average electron consumptions
442 in multiple electron addition tests for *Accumulibacter*_{nitrite} and *Accumulibacter*_{nitrate}
443 were 2.1 ± 0.63 and 2.47 ± 0.58 mmol e⁻ g VSS⁻¹ h⁻¹, respectively (Figure 4). These
444 values were higher than the total electron consumptions calculated for
445 *Accumulibacter*_{nitrite} with nitrite addition (test C, 1.44 mmol e⁻ gVSS⁻¹ h⁻¹) and for
446 *Accumulibacter*_{nitrate} with nitrate addition (test B, 2.36 mmol e⁻ gVSS⁻¹ h⁻¹). Thus,
447 despite the simultaneous presence of multiple electron acceptors, the PHA-derived
448 electron supply to denitrification enzymes increased as a function of the total NO_x
449 concentration, demonstrating that intracellular PHA storage was sufficient to support
450 denitrification in *Accumulibacter*.

451 Previously, it has been surmised that enzyme-specific affinity to electron
452 carriers and regulation of electron transfer are important factors that determine

453 electron distribution to enzymes involved in denitrification [28]. It is usually observed
454 that denitrification enzymes upstream (such as Nar) have a greater ability to receive
455 electron carriers than downstream enzymes (e.g. Nir and Nos) [46]. This is because
456 the ubiquinone/ubiquinol pool supplies electrons to the Nar enzymes and the
457 cytochrome c550/pseudoazurin pool, and the latter subsequently supplies electrons to
458 the Nir and Nos enzymes. In this study, *Accumulibacter*_{nitrate} and *Competibacter*
459 enrichments showed significantly higher electron consumption rates in batch test E
460 (NO_3^- and N_2O added) compared to batch test F (NO_2^- and N_2O added) (p-value =
461 0.007 and 0.044 for *Accumulibacter*_{nitrate} and *Competibacter*, respectively). However,
462 the trend for electron consumption was reversed for *Accumulibacter*_{nitrite} with electron
463 consumption in batch test F approximately 1.5 times that in test E (Figure 4) (p-value
464 = 0.028). Thus electron competition was not necessarily the limiting factor for
465 denitrification, enrichment-specific affinity for different electron acceptors also
466 affected the overall NO_x reduction. Further, in *Accumulibacter*_{nitrite} during nitrite
467 reduction, 37% of total electrons were distributed to nitrite reductase whereas in the
468 presence of other terminal electron acceptors, i.e., tests D, F and G, the fractions of
469 total electrons distributed to nitrite reductase were reduced to 30%, 27%, and 22%,
470 respectively. This proves that nitrite reductase did not display a higher ability to
471 compete for electrons compared to nitrate or nitrous oxide reductase, as has been
472 reported for heterotrophic organisms and some *Tetrasphaera*-related species [28, 42].

473 We also compared the phosphorus-uptake-to-electron-consumption ratio in all
474 batch tests of *Accumulibacter*_{nitrite} and *Accumulibacter*_{nitrate}, because the total electron
475 consumption is indicative of the energy utilized for anoxic phosphorus uptake (Figure
476 5). This ratio, just as the true denitrification rate, did not seem to be affected by
477 increasing concentrations of electron acceptors, but rather by the type of electron

478 acceptor present. Phosphorus uptake associated with nitrate in *Accumulibacter*_{nitrate}
479 enrichments was twice that observed for *Accumulibacter*_{nitrite}. Higher phosphorus
480 uptake was associated with nitrite and nitrous oxide compared to nitrate in
481 *Accumulibacter*_{nitrite} enrichments, emphasizing the impact of long-term adaptation to
482 certain terminal electron acceptors on observed denitrification kinetics and associated
483 phosphorus uptake.

484 In summary, the analysis of electron consumption and distribution in this
485 study leads to the conclusion that electron supply increased as a function of nitrogen
486 oxide concentration, indicating that adequate PHA levels can drive denitrification in
487 *Accumulibacter*. Upstream denitrification enzymes did not limit the flow of electrons
488 to Nos, and hence there was no electron competition for nitrous oxide reduction in
489 *Accumulibacter*. A comparison of the electron distribution in the two *Accumulibacter*
490 enrichments suggests an enrichment-specific affinity for terminal electron acceptors.

491

492 *3.5 Model evaluation of denitrification kinetics and electron competition*

493 The nitrate, nitrite, and nitrous oxide reduction rates for *Accumulibacter* measured
494 during the batch tests with low FNA inhibition were employed in a metabolic model
495 to predict anoxic growth at each denitrification step and the associated phosphorus
496 uptake for DPAOs [35]. The model used kinetic parameters specific for each step in
497 the denitrification process, and calculated a carbon oxidation rate to predict the
498 accumulation of denitrification products. As the flanking community members were
499 much less abundant than the *Accumulibacter* cells present in the enrichments, their
500 contribution to NO_x utilization was considered negligible. The model was optimized
501 by recalibrating four key kinetic parameters: rate constant for storage of
502 polyphosphate (q_{PP}), anoxic growth rate on nitrate (μ_{DPAO1}), anoxic growth rate on

503 nitrite (μ_{DPAO_2}) and anoxic growth rate on N_2O (μ_{DPAO_4}). In addition to these
504 parameters, another 17 kinetic and 6 stoichiometric parameters were obtained from
505 the literature (Table S1).

506 The optimized model captured the trends well for the reduction of various
507 nitrogen oxides (NO_x) and phosphorus uptake in the batch tests. The R^2 values
508 obtained for both *Accumulibacter* enrichments were 0.97 ± 0.01 , 0.96 ± 0.09 , $0.97 \pm$
509 0.05 and 0.96 ± 0.10 for nitrate, nitrite, N_2O and phosphorus, respectively, confirming
510 the robustness of the model and parameter values to accurately predict N_2O
511 accumulation in *Accumulibacter* enrichments (Figure 6). A comparison of the anoxic
512 growth rates optimized with the model revealed that the growth on nitrite, μ_{DPAO_2} , was
513 lower for *Accumulibacter*_{nitrate} compared to *Accumulibacter*_{nitrite}, indicating differences
514 in nitrite reducing abilities (p-value = 0.04). These observed differences also highlight
515 the effect of long-term adaptation to certain terminal electron acceptors.

516 In batch tests where N_2O was added in addition to nitrite or nitrate,
517 *Accumulibacter* effectively utilized N_2O that was produced from denitrification and,
518 more importantly, did not lead to any N_2O accumulation. A previous study reported a
519 similar observation for *Tetrasphaera*-related organisms, suggesting that high
520 availability of N_2O and energy from nitrate/nitrite reduction in these tests led to an
521 increased synthesis of nitrous oxide reductase (Nos) [42]. Here, we also used the
522 model to evaluate energy supplied for Nos synthesis (SI, Appendix 3, Table S6). For
523 *Accumulibacter*, the anoxic growth rate on N_2O increased approximately 1.5 to 2
524 times when multiple electron acceptors were added simultaneously (tests D to G) as
525 compared to tests with single terminal electron acceptors (tests A to C) (p-value =
526 0.03 and 0.0048 for *Accumulibacter*_{nitrite} and *Accumulibacter*_{nitrate}, respectively). This
527 further confirms our hypothesis that the increased availability of N_2O and energy

528 derived from the reduction of multiple electron acceptors allowed for the increase in
529 anoxic growth rate.

530 Other mathematical models have been used to predict phosphorus removal,
531 but few compared the nitrous oxide (N₂O) accumulation from denitrifying phosphorus
532 removal processes. A limitation is that the denitrification process is usually
533 represented as a single- or two-step process. One study utilized a similar four-step
534 denitrification model as our approach to predict nitrous oxide (N₂O) accumulation
535 during biological nitrogen removal in anaerobic/anoxic/oxic sequencing batch
536 reactors (A²O-SBR), but abstained from accounting for the abundant *Accumulibacter*
537 and *Competibacter* organisms usually found in these systems [47]. It can be surmised
538 that lack of organism-specific parameters in the model can lead to a lower precision
539 of N₂O accumulation prediction. In contrast, the model applied in this study lacks the
540 aforementioned shortcomings and adequately describes N₂O accumulation during
541 denitrification [35].

542 The model heuristic can also be integrated with other N₂O models for
543 nitrification and denitrification to gain more insight into N₂O dynamics during various
544 stages of biological wastewater treatment. FNA concentrations kept below inhibitory
545 levels in this study allowed for modelling of the true denitrification kinetics in
546 *Accumulibacter*. FNA inhibition leading to N₂O accumulation is not limited to
547 polyphosphate accumulating organisms, but has also been documented for
548 heterotrophic, hydrogenotrophic, ammonia-oxidising and Anammox organisms [48-
549 51]. A lower tendency for N₂O accumulation and higher anoxic growth rate on N₂O
550 was observed when FNA concentrations were low. This identifies FNA as an
551 important parameter that must be included in models developed to predict N₂O
552 accumulation based on nitrite concentration and pH. To supplement these modelling

553 predictions, future studies can also include metatranscriptomic analysis of the
554 denitrification enzymes in *Accumulibacter*, and compare levels of transcription at
555 different FNA concentrations.

556

557 **4. CONCLUSIONS**

558 Denitrifying phosphorus removal (DPR) is a promising technology. In this work we
559 have focussed on the potential for nitrous oxide accumulation by dominant microbial
560 community members - *Accumulibacter* and *Competibacter* - in DPR systems. Our
561 batch test results and validation with a metabolic model suggest that denitrification by
562 *Accumulibacter* and *Competibacter* is not limited by electron competition. In fact in
563 *Accumulibacter*, anoxic growth on nitrous oxide (N₂O) in the presence of other
564 nitrogen oxides was significantly higher compared to when nitrous oxide added as
565 sole electron acceptor. Our observations indicate that sufficiently high PHA levels
566 and low free nitrous acid (FNA) inhibition resulted in increased transcription of the
567 *nos* gene, allowing for higher N₂O reduction than previously observed. The
568 denitrification kinetics for *Competibacter* revealed poor nitrite or nitrous oxide
569 utilization despite sufficient PHA storage and low FNA inhibition, implying a
570 truncated denitrification pathway. To conclude, the reduction of nitrogen oxides by
571 *Accumulibacter* and *Competibacter* is largely governed by their denitrification
572 enzyme-specific affinity to electron carriers, the availability of sufficient internal
573 storage polymers to provide energy for electron transfer and low concentrations of
574 FNA. Understanding the nitrous oxide reduction potential of the dominant microbial
575 community members in DPR can be leveraged to design energy efficient treatment
576 processes for biological phosphorus removal and subsequently reduce unwanted
577 emissions.

578

579 **AUTHOR CONTRIBUTIONS**

580 The study was designed by SR, SW and HYN. SR conducted the batch test
581 experiments and analysed the microbial community. SR, NP and SW analysed and
582 interpreted the data obtained over the course of this study and wrote the manuscript
583 with contributions from HYN.

584

585 **ACKNOWLEDGEMENTS**

586 This research was supported by the Ministry of Education, Singapore under the
587 Research Centre of Excellence Programme. We acknowledge Dr. Daniela Drautz-
588 Moses for performing 16S rRNA gene amplicon sequencing. Many thanks go to Dr.
589 Rohan Williams for his inputs on interpretation of the sequencing data and for
590 proofreading the manuscript. We also extend our gratitude to James Jun, Muhamad
591 Danial Bin Suthree, Ahmadul Hafiz Ain Azman Jun, Eganathan Kaliyamoorthy and
592 Sara Swa Thi for performing nutrient tests during the course of this study.

593

594 **REFERENCES**

- 595 [1] Energy Conservation in Water and Wastewater Treatment Facilities Task Force
596 Water Environment Federation, Energy conservation in water and wastewater
597 treatment facilities, WEF Press, McGraw Hill companies, Alexandria, VA, USA,
598 2009.
- 599 [2] G. Tchobanoglous, F. L., Burton, H. D. Stensel, Metcalf & Eddy Inc., Wastewater
600 engineering; treatment and reuse, McGraw-Hill Education 2003.
- 601 [3] J.P. Kern-Jespersen, Mogens, H., Biological phosphorus uptake under anoxic and
602 aerobic conditions, *Water Res* 27 (1993) 617-624.
- 603 [4] G. Carvalho, P. C. Lemos, A. Oehmen, M. A. M. Reis, Denitrifying phosphorus
604 removal: Linking the process performance with the microbial community structure,
605 *Water Res* 41 (2007) 4383-4396.
- 606 [5] G. Qiu, R. Zuniga-Montanez, Y. Law, S.S. Thi, T.Q.N. Nguyen, K. Eganathan, X.
607 Liu, P.H. Nielsen, R.B.H. Williams, S. Wuertz, Polyphosphate-accumulating
608 organisms in full-scale tropical wastewater treatment plants use diverse carbon
609 sources, *Water Res* 149 (2019) 496-510.
- 610 [6] L.C. Burow, Y. Kong, N.J. L., B.L. L., P.H. Nielsen, Abundance and
611 ecophysiology of *Defluviicoccus* spp., glycogen-accumulating organisms in full-scale

- 612 wastewater treatment processes, *Microbiology* (Reading, England) 153 (2007) 178-
613 185.
- 614 [7] S.J.A. McIlroy, E.K. M. Andresen, A.M. Saunders, R. Kristiansen, M. Stokholm
615 Bjerregaard, K.L. Nielsen, P.H. Nielsen, '*Candidatus* Competibacter'-lineage genomes
616 retrieved from metagenomes reveal functional metabolic diversity, *Isme J* 8 (2014)
617 613-624.
- 618 [8] T. Nittami, S. McIlroy, E.M. Seviour, S. Schroeder, R.J. Seviour, *Candidatus*
619 *Monilibacter* spp., common bulking filaments in activated sludge, are members of
620 Cluster III *Defluviicoccus*, *Syst Appl Microbiol* 32 (2009) 480-489.
- 621 [9] A. Oehmen, A.M. Saunders, M.T. Vives, Z. Yuan, J. Keller, Competition between
622 polyphosphate and glycogen accumulating organisms in enhanced biological
623 phosphorus removal systems with acetate and propionate as carbon sources, *J*
624 *Biotechnol* 123 (2006) 22-32.
- 625 [10] R.A. Sanford, D.D. Wagner, Q. Wu, J.C. Chee-Sanford, S.H. Thomas, C. Cruz-
626 García, G. Rodríguez, A. Massol-Deyá, K.K. Krishnani, K.M. Ritalahti, S. Nissen,
627 K.T. Konstantinidis, F.E. Löffler, Unexpected nondenitrifier nitrous oxide reductase
628 gene diversity and abundance in soils, *Proc Natl Acad Sci* 109 (2012) 19709-19714.
- 629 [11] D.R.J. Graf, C. M. Hallin, S., Intergenomic comparisons highlight modularity of
630 the denitrification pathway and underpin the importance of community structure for
631 N₂O emissions, *PloS one* 9 (2014) e114118.
- 632 [12] C.M. Jones, D.R. Graf, D. Bru, L. Philippot, S. Hallin, The unaccounted yet
633 abundant nitrous oxide-reducing microbial community: a potential nitrous oxide sink,
634 *Isme J* 7 (2013) 417-426.
- 635 [13] R.J. Zeng, R. Lemaire, Z. Yuan, J. Keller, Simultaneous nitrification,
636 denitrification, and phosphorus removal in a lab-scale sequencing batch reactor,
637 *Biotechnol Bioeng* 84 (2003) 170-178.
- 638 [14] R.J. Zeng, Z. Yuan, J. Keller, Enrichment of denitrifying glycogen-accumulating
639 organisms in anaerobic/anoxic activated sludge system, *Biotechnol Bioeng* 81 (2003)
640 397-404.
- 641 [15] C.T.B. Skennerton, J. J. Slater, F. R. Bond, P. L. Tyson, G. W., Expanding our
642 view of genomic diversity in *Candidatus* *Accumulibacter* clades, *Environ Microbiol*
643 17 (2015) 1574-1585.
- 644 [16] P.Y. Camejo, B.O. Oyserman, K.D. McMahon, D.R. Noguera, Integrated omic
645 analyses provide evidence that a "*Candidatus* *Accumulibacter phosphatis*" strain
646 performs denitrification under microaerobic conditions, *MSYSTEMS* 4 (2019)
647 e00193-00118.
- 648 [17] S. He, V. Kunin, M. Haynes, H.G. Martin, N. Ivanova, F. Rohwer, P.
649 Hugenholtz, K.D. McMahon, Metatranscriptomic array analysis of '*Candidatus*
650 *Accumulibacter phosphatis*'-enriched enhanced biological phosphorus removal
651 sludge, *Environ Microbiol* 12 (2010) 1205-1217.
- 652 [18] T. Mino, L. Wen-Tso, K. Futoshi, M. Tomonori, Modelling glycogen storage and
653 denitrification capability of microorganisms in enhanced biological phosphate
654 removal processes, *Water Sci Technol* 31 (1995) 25-34.
- 655 [19] M.T. Wong, W.T. Liu, Ecophysiology of *Defluviicoccus*-related tetrad-forming
656 organisms in an anaerobic-aerobic activated sludge process, *Environ Microbiol* 9
657 (2007) 1485-1496.
- 658 [20] Z. Wang, F. Guo, Y. Mao, Y. Xia, T. Zhang, Metabolic characteristics of a
659 glycogen-accumulating organism in *Defluviicoccus* cluster II revealed by comparative
660 genomics, *Microb Ecol* 68 (2014) 716-728.

- 661 [21] M. Henze, W. Gujer, T. Mino, T. Matsuo, M.C. Wentzel, G.v.R. Marais, M.C.
662 Van Loosdrecht, Activated sludge model no. 2d, ASM2d, *Water Sci Technol* 39
663 (1999) 165-182.
- 664 [22] Z.r. Hu, M. Wentzel, G. Ekama, A general kinetic model for biological nutrient
665 removal activated sludge systems: model development, *Biotechnol Bioeng* 98 (2007)
666 1242-1258.
- 667 [23] P. Barker, P. Dold, General model for biological nutrient removal activated-
668 sludge systems: model presentation, *Water Environ Res* 69 (1997) 969-984.
- 669 [24] M.J. Kampschreur, H. Temmink, R. Kleerebezem, M.S.M. Jetten, M.C.M. van
670 Loosdrecht, Nitrous oxide emission during wastewater treatment, *Water Res* 43
671 (2009) 4093-4103.
- 672 [25] H. Itokawa, K. Hanaki, T. Matsuo, Nitrous oxide production in high-loading
673 biological nitrogen removal process under low COD/N ratio condition, *Water Res* 35
674 (2001) 657-664.
- 675 [26] Y. Zhou, M. Pijuan, R.J. Zeng, Z. Yuan, Free nitrous acid inhibition on nitrous
676 oxide reduction by a denitrifying-enhanced biological phosphorus removal sludge,
677 *Environ Sci Technol* 42 (2008) 8260-8265.
- 678 [27] A. Vieira, C.F. Galinha, A. Oehmen, G. Carvalho, The link between nitrous
679 oxide emissions, microbial community profile and function from three full-scale
680 WWTPs, *Sci Total Environ* 651 (2019) 2460-2472.
- 681 [28] Y. Pan, B.J. Ni, P.L. Bond, L. Ye, Z. Yuan, Electron competition among nitrogen
682 oxides reduction during methanol-utilizing denitrification in wastewater treatment,
683 *Water Res* 47 (2013) 3273-3281.
- 684 [29] D. Richardson, H. Felgate, N. Watmough, A. Thomson, E. Baggs, Mitigating
685 release of the potent greenhouse gas N₂O from the nitrogen cycle - could enzymic
686 regulation hold the key?, *Trends Biotechnol* 27 (2009) 388-397.
- 687 [30] R. Lemaire, R. Meyer, A. Taske, G.R. Crocetti, J. Keller, Z. Yuan, Identifying
688 causes for N₂O accumulation in a lab-scale sequencing batch reactor performing
689 simultaneous nitrification, denitrification and phosphorus removal, *J Biotechnol* 122
690 (2006) 62-72.
- 691 [31] Y. Zhou, M. Lim, S. Harjono, W.J. Ng, Nitrous oxide emission by denitrifying
692 phosphorus removal culture using polyhydroxyalkanoates as carbon source, *Int J*
693 *Environ Sci* 24 (2012) 1616-1623.
- 694 [32] J.M. Santos, L. Rieger, A.B. Lanham, M. Carvalheira, M.A. Reis, A. Oehmen, A
695 novel metabolic-ASM model for full-scale biological nutrient removal systems, *Water*
696 *Res* 171 (2020) 115373.
- 697 [33] B.-J. Ni, M. Ruscalleda, C. Pellicer-Nàcher, B.F. Smets, Modeling nitrous oxide
698 production during biological nitrogen removal via nitrification and denitrification:
699 Extensions to the general ASM models, *Environ Sci Technol* 45 (2011) 7768-7776.
- 700 [34] T. Kuba, E. Murnleitner, M. Van Loosdrecht, J. Heijnen, A metabolic model for
701 biological phosphorus removal by denitrifying organisms, *Biotechnol Bioeng* 52
702 (1996) 685-695.
- 703 [35] Y. Liu, L. Peng, X. Chen, B.-J. Ni, Mathematical modeling of nitrous oxide
704 production during denitrifying phosphorus removal process, *Environ Sci Technol* 49
705 (2015) 8595-8601.
- 706 [36] A. Ribera-Guardia, R. Marques, C. Arangio, M. Carvalheira, A. Oehmen, M.
707 Pijuan, Distinctive denitrifying capabilities lead to differences in N₂O production by
708 denitrifying polyphosphate accumulating organisms and denitrifying glycogen
709 accumulating organisms, *Bioresour Technol* 219 (2016) 106-113.

- 710 [37] A. Oehmen, C.M.C. Lopez-Vazquez, G. Reis, M. C. van Loosdrecht, , Modelling
711 the population dynamics and metabolic diversity of organisms relevant in
712 anaerobic/anoxic/aerobic enhanced biological phosphorus removal processes, *Water*
713 *Res* 44 (2010) 4473-4486.
- 714 [38] G. Guo, Y. Wang, C. Wang, H. Wang, M. Pan, S. Chen, Short-term effects of
715 excessive anaerobic reaction time on anaerobic metabolism of denitrifying
716 polyphosphate-accumulating organisms linked to phosphorus removal and N₂O
717 production, *Front Env Sci Eng* 7 (2013) 616-624.
- 718 [39] S. Otte, N.G. Grobben, L.A. Robertson, M. Jetten, J.G. Kuenen, Nitrous oxide
719 production by *Alcaligenes faecalis* under transient and dynamic aerobic and anaerobic
720 conditions, *Appl Environ Microbiol* 62 (1996) 2421-2426.
- 721 [40] Y. Wei, S. Wang, B. Ma, X. Li, Z. Yuan, Y. He, Y. Peng, The effect of poly-
722 beta-hydroxyalkanoates degradation rate on nitrous oxide production in a denitrifying
723 phosphorus removal system, *Bioresour Technol* 170 (2014) 175-182.
- 724 [41] N. Adouani, T. Lendormi, L. Limousy, O. Sire, Effect of the carbon source on
725 N₂O emissions during biological denitrification, *Resour Conserv Recycl* 54 (2010)
726 299-302.
- 727 [42] R. Marques, A. Ribera-Guardia, J. Santos, G. Carvalho, M.A.M. Reis, M. Pijuan,
728 A. Oehmen, Denitrifying capabilities of *Tetrasphaera* and their contribution towards
729 nitrous oxide production in enhanced biological phosphorus removal processes, *Water*
730 *Res* 137 (2018) 262-272.
- 731 [43] X.Z. Han Gao, Lei Zhou, Fabrizio Sabba, George F. Wells, Differential kinetics
732 of nitrogen oxides reduction leads to elevated nitrous oxide production by a nitrite fed
733 granular denitrifying EBPR bioreactor *Environmental Science: Water Research &*
734 *Technology*, (2020).
- 735 [44] B. Baumann, J.R. van der Meer, M. Snozzi, A.J. Zehnder, Inhibition of
736 denitrification activity but not of mRNA induction in *Paracoccus denitrificans* by
737 nitrite at a suboptimal pH, *Anton Leeuw Int J G* 72 (1997) 183-189.
- 738 [45] T. Rasmussen, T. Brittain, B.C. Berks, N.J. Watmough, A.J. Thomson,
739 Formation of a cytochrome-c nitrous oxide reductase complex is obligatory for N₂O
740 reduction by *Paracoccus pantotrophus*, *Dalton Trans* (2005) 3501-3506.
- 741 [46] M.R. Betlach, J.M. Tiedje, Kinetic explanation for accumulation of nitrite, nitric
742 oxide, and nitrous oxide during bacterial denitrification, *Appl Environ Microbiol* 42
743 (1981) 1074-1084.
- 744 [47] X. Ding, J. Zhao, B. Hu, X. Li, G. Ge, K. Gao, Y. Chen, Mathematical modeling
745 of nitrous oxide (N₂O) production in anaerobic/anoxic/oxic processes: Improvements
746 to published N₂O models, *Chem Eng* 325 (2017) 386-395.
- 747 [48] Y. Wang, P. Li, J. Zuo, Y. Gong, S. Wang, X. Shi, M. Zhang, Inhibition by free
748 nitrous acid (FNA) and the electron competition of nitrite in nitrous oxide (N₂O)
749 reduction during hydrogenotrophic denitrification, *Chemosphere* 213 (2018) 1-10.
- 750 [49] C.T. Kinh, J. Ahn, T. Suenaga, N. Sittivorakulpong, P. Noophan, T. Hori, S.
751 Riya, M. Hosomi, A. Terada, Free nitrous acid and pH determine the predominant
752 ammonia-oxidizing bacteria and amount of N₂O in a partial nitrifying reactor, *Appl*
753 *Microbiol Biotechnol* 101 (2017) 1673-1683.
- 754 [50] Q. Wang, G. Jiang, L. Ye, M. Pijuan, Z. Yuan, Heterotrophic denitrification
755 plays an important role in N₂O production from nitrification reactors treating anaerobic
756 sludge digestion liquor, *Water Res* 62 (2014) 202-210.
- 757 [51] N. Pradhan, Swa Thi, Sara., Wuertz Stefan., Inhibition factors and kinetic model
758 for anaerobic ammonia oxidation in a granular sludge bioreactor with *Candidatus*
759 *Brocadia*, *Chem Eng* 389: (2020) 123618.

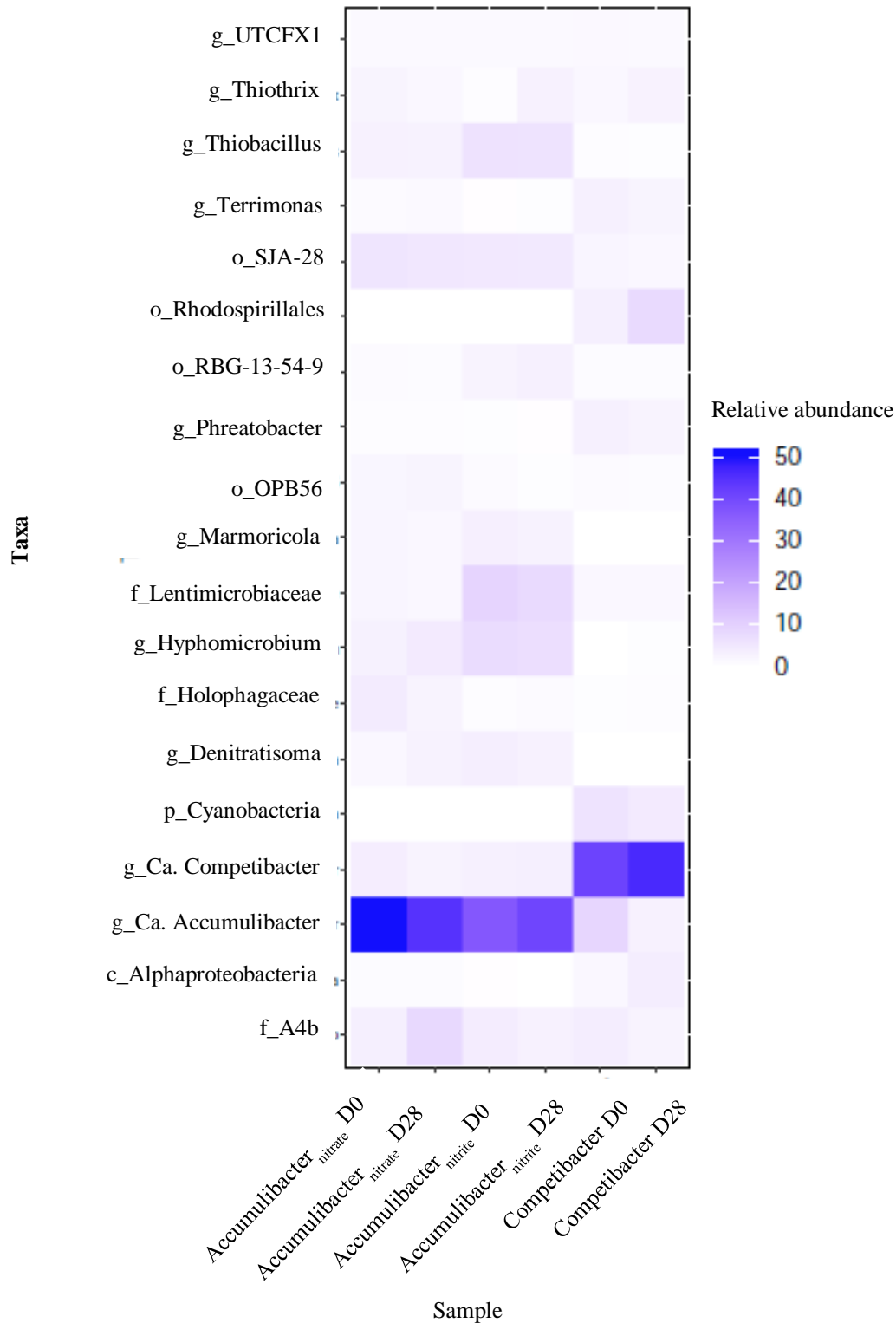
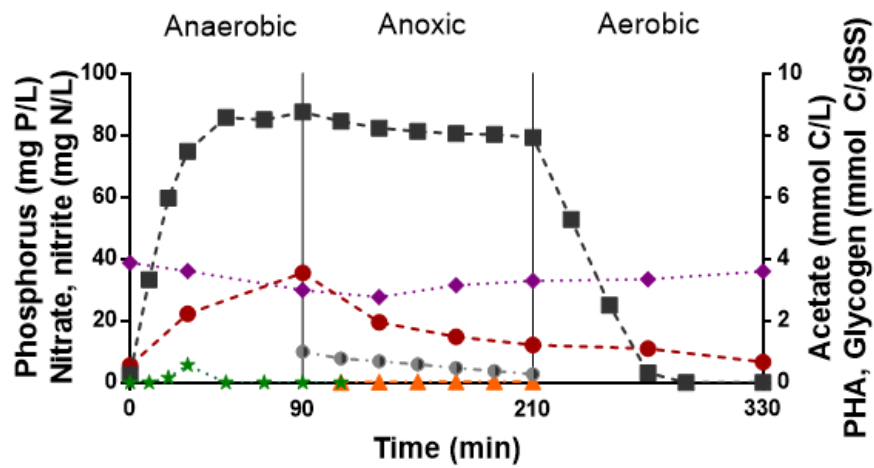


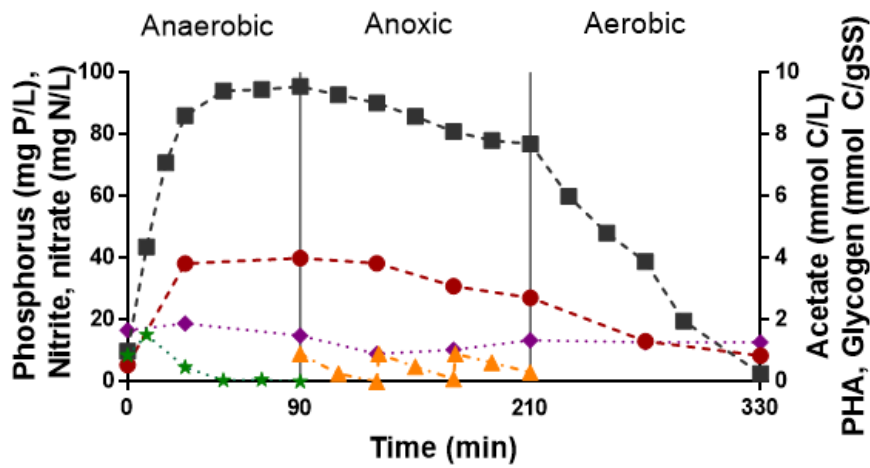
Figure 1. Microbial community analysis for samples collected at the start (D0) and end (D28) of batch tests from *Accumulibacter*_{nitrite}, *Accumulibacter*_{nitrate}, and *Competibacter* enrichment. Shown are the 15 most abundant organisms based on 16S rRNA gene amplicon sequencing and classified by the highest level of resolution obtained for each V1-V3 ASV annotated using the SILVA database. The microbial

community was dominated by the respective target organism for each reactor and the abundance remained stable during the course of the experiment.

(a)



(b)



(c)

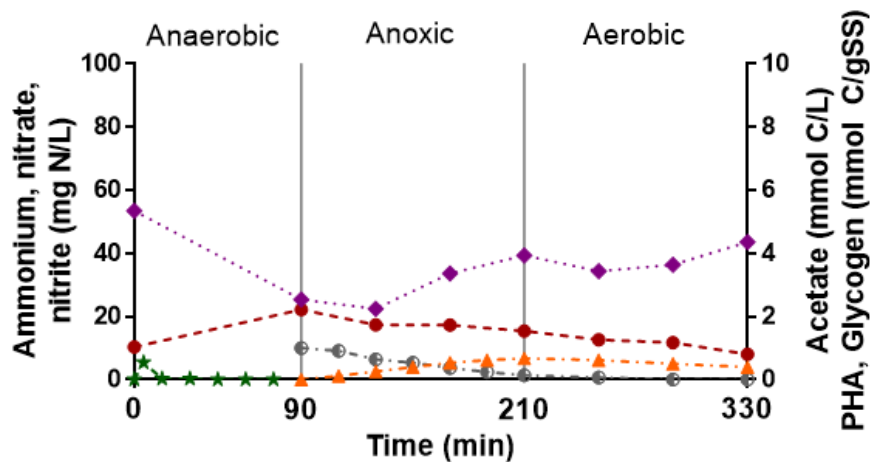
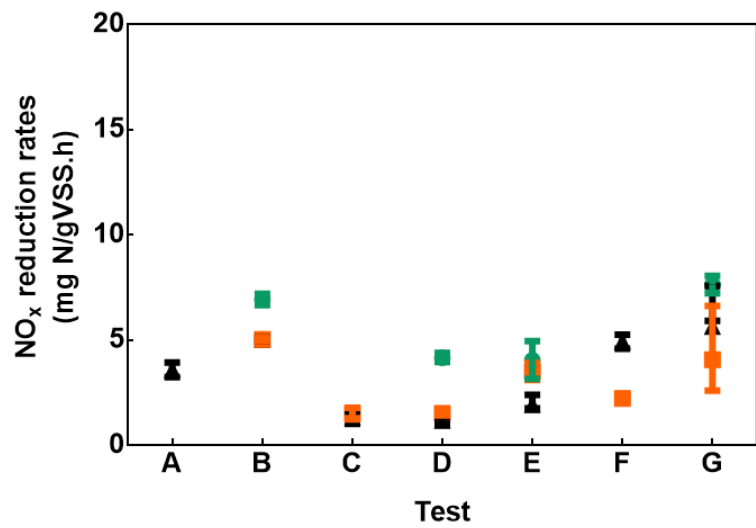
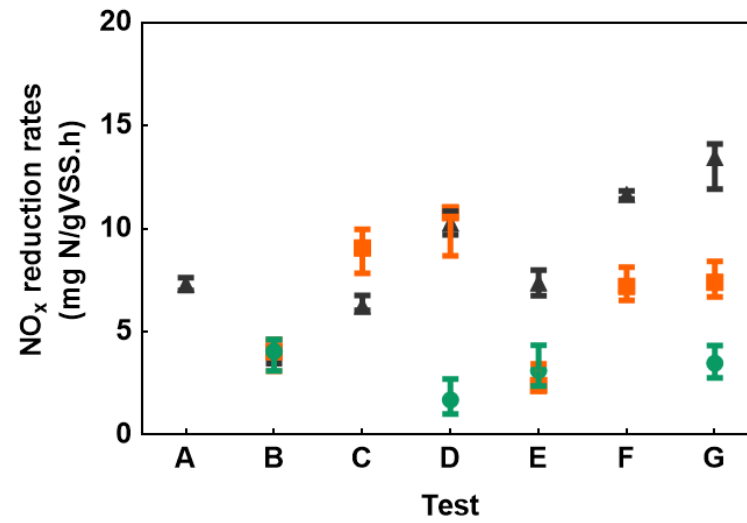
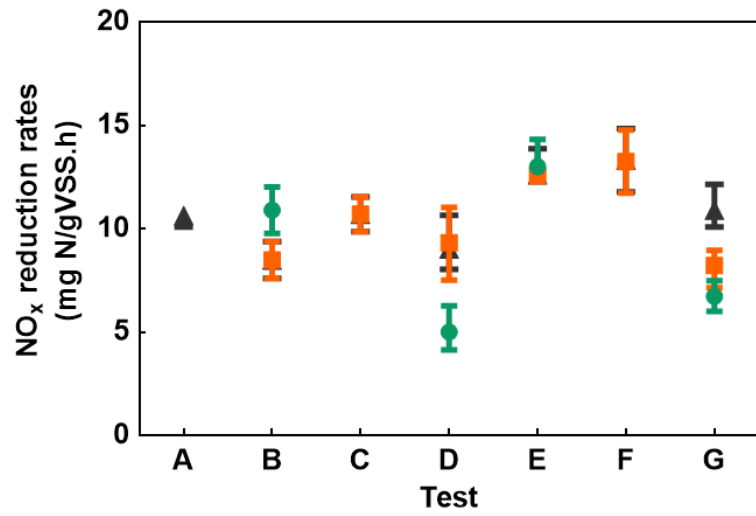
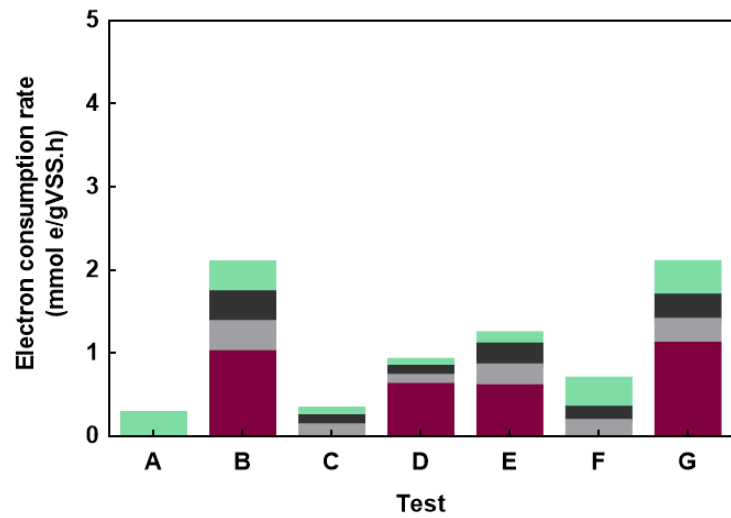
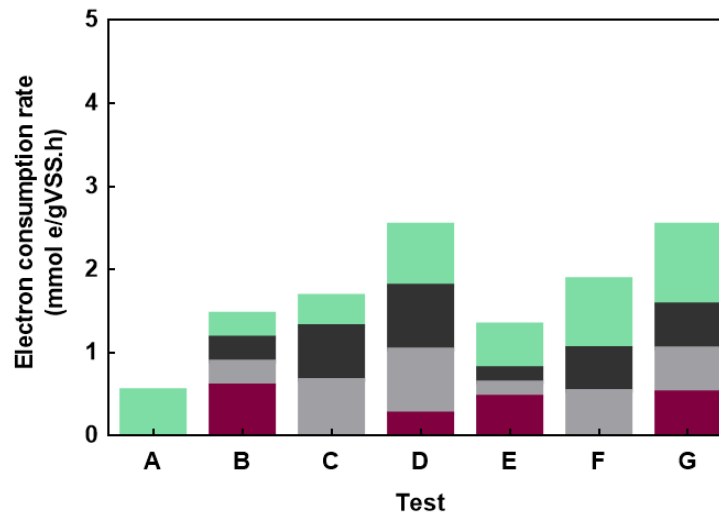
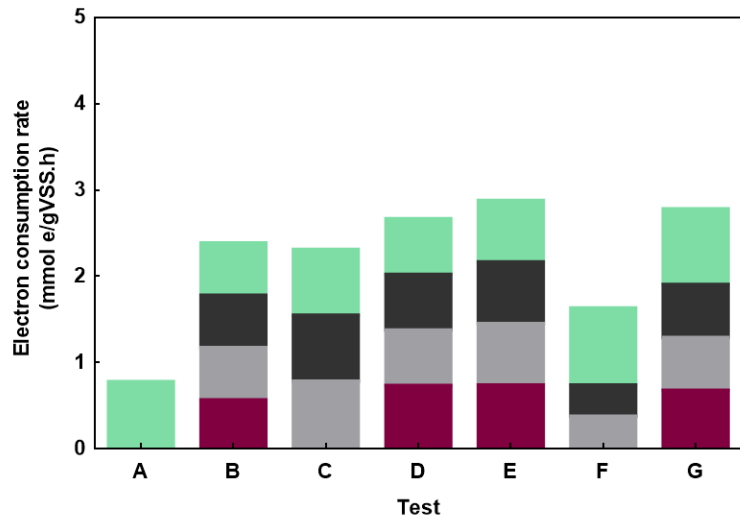


Figure 2. Transformation of nutrients and intracellular storage compounds during a typical SBR cycle of (a) *Accumulibacter*_{nitrate}, (b) *Accumulibacter*_{nitrite}, and (c) *Competibacter*.



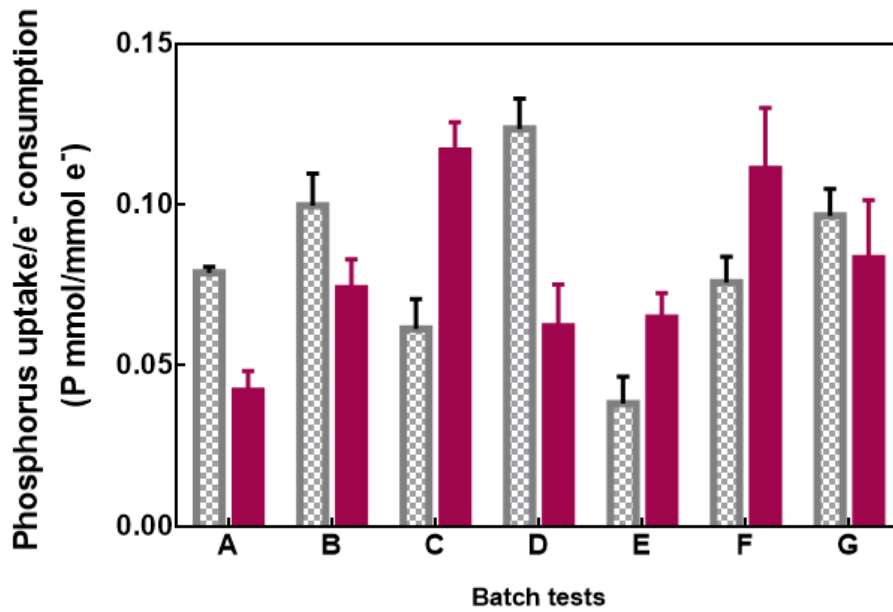
Batch test	Electron acceptor added
A	N_2O
B	NO_3^-
C	NO_2^-
D	NO_3^- , NO_2^-
E	NO_3^- , N_2O
F	NO_2^- , N_2O
G	NO_3^- , NO_2^- , N_2O

Figure 3. True reduction rate of nitrate, nitrite and N₂O in batch test conditions A to G for (a) *Accumulibacter*_{nitrate} (b) *Accumulibacter*_{nitrite}, and (c) *Competibacter* enrichments. The mean and range shown here were obtained from two replicates.



Batch test	Electron acceptor added
A	N_2O
B	NO_3^-
C	NO_2^-
D	NO_3^- , NO_2^-
E	NO_3^- , N_2O
F	NO_2^- , N_2O
G	NO_3^- , NO_2^- , N_2O

Figure 4. Electron consumption rates by specific denitrification enzymes for batch test conditions A to G for (a) *Accumulibacter*_{nitrate}, (b) *Accumulibacter*_{nitrite}, and (c) *Competibacter*. Denitrification enzymes are nitrate reductase (Nar, shown in maroon), nitrite reductase (Nir, in grey), nitric oxide reductase (Nor, in black) and nitrous oxide reductase (Nos, in green).



	Batch test	Electron acceptor added
	A	N ₂ O
	B	NO ₃ ⁻
☒ Accumulibacter _{nitrate}	C	NO ₂ ⁻
■ Accumulibacter _{nitrite}	D	NO ₃ ⁻ , NO ₂ ⁻
	E	NO ₃ ⁻ , N ₂ O
	F	NO ₂ ⁻ , N ₂ O
	G	NO ₃ ⁻ , NO ₂ ⁻ , N ₂ O

Figure 5. Ratio of P uptake per electron consumption (mmol e⁻) obtained for the batch tests performed with various terminal electron acceptors for the two Accumulibacter enrichment cultures – Accumulibacter_{nitrite} and Accumulibacter_{nitrate}.

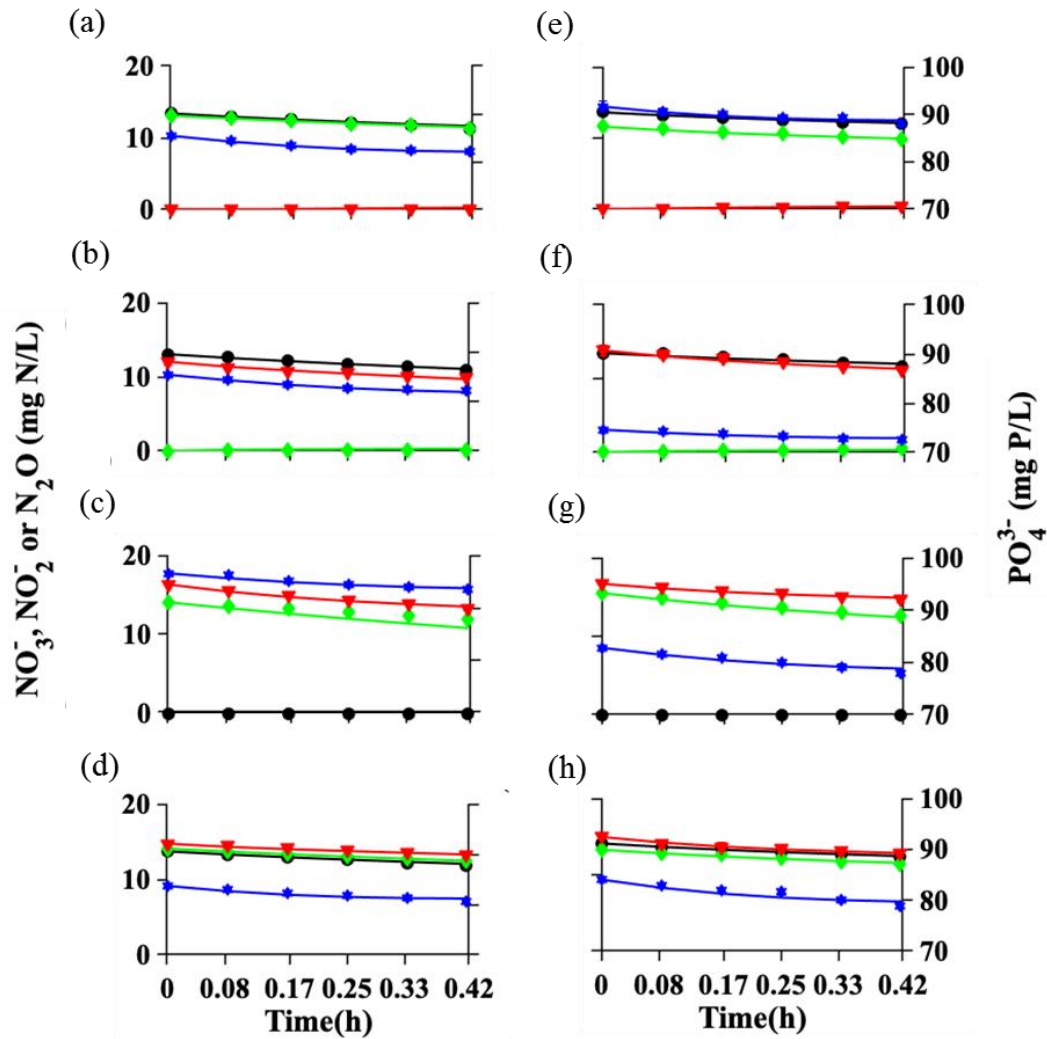


Figure 6. Simulation of batch perturbation studies of nitrate-enriched *Accumulibacter* with (a) NO_3^- and NO_2^- , (b) NO_3^- and N_2O , (c) NO_2^- and N_2O , and (d) NO_3^- , NO_2^- and N_2O . Simulation of batch perturbation study of nitrite-enriched *Accumulibacter* with (e) with NO_3^- and NO_2^- , (f) NO_3^- and N_2O , (g) NO_2^- and N_2O , and (h) with NO_3^- , NO_2^- and N_2O . x_axis limit (0 – 0.42), y_axis_left limit (0 – 20) and y_axis_right limit (70 – 90). Figure legend: predicted PO_4^{3-} (—, solid blue line), predicted NO_3^- (—, solid black line), predicted NO_2^- (—, solid green line), predicted N_2O (—, solid red line), measured PO_4^{3-} (★), measured NO_3^- (●), measured NO_2^- (◆), and measured N_2O (▼).

Table 1. Electron acceptors added in different batch tests

Batch test	Electron acceptor	Intermediate measured
A	N ₂ O	N ₂ O
B	NO ₃ ⁻	NO ₃ ⁻ , NO ₂ ⁻ , N ₂ O
C	NO ₂ ⁻	NO ₂ ⁻ , N ₂ O
D	NO ₃ ⁻ , NO ₂ ⁻	NO ₃ ⁻ , NO ₂ ⁻ , N ₂ O
E	NO ₃ ⁻ , N ₂ O	NO ₃ ⁻ , NO ₂ ⁻ , N ₂ O
F	NO ₂ ⁻ , N ₂ O	NO ₂ ⁻ , N ₂ O
G	NO ₃ ⁻ , NO ₂ ⁻ , N ₂ O	NO ₃ ⁻ , NO ₂ ⁻ , N ₂ O

Table 2. Comparison of the amount of N₂O accumulated per N reduced (in mg/L) with values in previous studies

Study	FNA level calculated (HNO ₂ -N. L ⁻¹)	Batch test (electron acceptor added)					
		Test B (NO ₃ ⁻)	Test C (NO ₂ ⁻)	Test D (NO ₂ ⁻ & NO ₃ ⁻)	Test E (NO ₃ ⁻ & N ₂ O)	Test F (NO ₂ ⁻ & N ₂ O)	Test G (NO ₂ ⁻ , NO ₃ ⁻ & N ₂ O)
Acc ^a	0.1 - 0.2 µg	0.31 ± 0.01	6.93 ± 0.38	3.63 ± 0.18	-	-	-
Acc ^b	0.1 - 0.2 µg	-	30.97 ± 1.06	8.40 ± 0.01	-	-	-
Comp ^c	0.1 - 0.2 µg	-	15.83 ± 2.59	1.07 ± 0.97	1.57 ± 0.26	-	-
Tet ^d	5 µg	16.7 ± 0.8	15.5 ± 0.8	17.7 ± 0.9	-	-	-
DPAO ^e	1.58 µg	8.72 ± 0.2	17.4 ± 5.9	31.2 ± 2.70	-	20.11 ± 1.90	11.30 ± 3.10
DGAO ^f	1.58 µg	7.12 ± 2.16	82.95 ± 4.79	45.45 ± 0.89	13.71 ± 5.81	56.90 ± 4.92	48.45 ± 5.94

^a *Ca. Accumulibacter* (enriched with nitrate as terminal electron acceptor in this study) (this study)

^b *Ca. Accumulibacter* (enriched with nitrate as terminal electron acceptor in this study) (this study)

^c *Ca. Competibacter* (enriched with nitrate as terminal electron acceptor in this study)

^d *Tetrasphaera* culture (Marques et al. 2018)

^e DPAO culture (*Accumulibacter* clade I and II present) (Ribera et al., 2016)

^f DGAO culture (*Competibacter* and *Defluviicoccus* present) (Ribera et al., 2016)

- Below detection limit

Table 3. Mean PHA concentration and standard deviation at the beginning and end of batch tests

Enrichment	Phase	Batch test (electron acceptor added)						
		Test A (N ₂ O)	Test B (NO ₃ ⁻)	Test C (NO ₂ ⁻)	Test D (NO ₂ ⁻ & NO ₃ ⁻)	Test E (NO ₃ ⁻ & N ₂ O)	Test F (NO ₂ ⁻ & N ₂ O)	Test G (NO ₂ ⁻ , NO ₃ ⁻ & N ₂ O)
Accumulibacter _{nitrate}	Start (90 min)	10.59 ± 1.58	7.16 ± 1.09	7.37 ± 0.16	8.60 ± 0.80	8.74 ± 1.02	9.14 ± 0.01	6.07 ± 0.39
	End (120 min)	9.54 ± 0.57	5.71 ± 1.13	6.09 ± 0.08	6.13 ± 0.10	4.77 ± 0.82	6.64 ± 0.71	3.80 ± 0.23
Accumulibacter _{nitrite}	Start (90 min)	6.57 ± 0.44	10.06 ± 0.33	10.75 ± 0.97	9.97 ± 0.07	10.15 ± 0.31	13.88 ± 0.34	7.64 ± 0.51
	End (120 min)	5.67 ± 0.96	9.43 ± 0.88	9.18 ± 1.60	8.89 ± 0.15	9.07 ± 0.52	12.67 ± 0.60	7.21 ± 0.49
Competibacter	Start (90 min)	5.03 ± 0.91	8.16 ± 1.06	6.23 ± 0.34	9.97 ± 1.14	7.96 ± 0.29	6.16 ± 0.16	8.16 ± 0.07
	End (120 min)	4.04 ± 1.21	7.66 ± 0.32	6.52 ± 0.08	8.12 ± 0.76	6.19 ± 0.15	5.63 ± 0.02	6.36 ± 0.14